RSC Advances

Kinetic study of self-assembly Ni(II)-doped TiO2 nanocatalysts for the photodegradation of azo pollutants

Journal:	*RSC Advances*
Manuscript ID	RA-ART-08-2015-016172.R1
Article Type:	Paper
Date Submitted by the Author:	29-Sep-2015
Complete List of Authors:	Chen, Chia-Yun; National Chi Nan University, Department of Applied Materials and Optoelectronic Engineering Hsu, Li-Jen; National Chi Nan University, Department of Applied Materials and Optoelectronic Engineering
Subject area & keyword:	

Journal Name

ARTICLE

Kinetic study of self-assembly Ni(II)-doped TiO_2 nanocatalysts for the photodegradation of azo pollutants

Received 00th January 20xx,
Accepted 00th January 20xx

DOI: 10.1039/x0xx00000x

www.rsc.org/

Chia-Yun Chen* and Li-Jen Hsu

Ni(II)-doped TiO_2 nanoparticles were fabricated by a simple and reliable hydrothermal method. Morphology, crystallographic structure and light-absorption property of the formed photocatalysts were characterized. In addition, both the adsorption phenomena and photodegradation of two types of azo dyes in the presence of Ni(II)-doped TiO_2 were investigated. The experimental results showed that the dye adsorption follows the Langmuir adsorption pathway, and the dye degradation was significantly enhanced by doping of Ni ions into TiO_2 photocatalysts. The optimal doping of Ni ions for the removal of RB5 and 3R dyes was found to be 1 %, giving the degradation efficiency of 3 times for RB5 dyes and 3.5 times for 3R dyes higher than those of un-doped TiO_2. Furthermore, the underlying kinetic mechanism was systematically studied, in which the second-order kinetic model was found to be the explicit mechanism for dye degradation on TiO_2 with Ni(II) doping.

Introduction

Azo dyes, primarily from the effluent discharge of textile industry, are regarded as one of the most hazardous sources of environmental contamination.[1] Unfortunately, these noxious materials released with water effluents, are remarkably stable and non-biodegradable.[1,2] Therefore, once they are discharged inappropriately or under careless effluent treatments, the resulting wastewater may cause serious destruction to the living environment. Apart from that, the by-products are often toxic, mutagenic, and carcinogenic, which are harmful to aquatic animals, microorganisms, human beings and even to the entire ecosystem.[3] It is therefore essential to well treat these effluents prior to discharging them into various water bodies. During the last decade, Titanium dioxide (TiO_2) has been widely investigated for the efficient degradation of such water pollutants, mainly because of their excellent photocatalytic activity, low production cost, non-toxicity and robust chemical stability.[4]

To further improve their performances on dye degradation, recent studies are extensively focused on the incorporation of metal ions with TiO_2 photocatalysts,[5-7] or the formation of heterostructured photocatalysts,[8, 9] the promising pathways for both giving the visible-light photocatalytic response and enhancing the effective charge transfer of photo-generated carriers upon photocatalysis process. So far, many methods have been made to prepare metal-ion doped TiO_2, such as sol-gel process,[10] ion impregnation[11] and hydrothermal method[12] and others. Nevertheless, the low photocatalytic efficiency of doped TiO_2 catalysts prepared with sol-gel method was usually encountered, mainly resulting from the uneven formation or segregation of metal ions on TiO_2 lattices. On the other hand, ion impregnation method also suffered the non-uniform doping process since substitution of metal ions preferentially occurs at TiO_2 surfaces instead of entire TiO_2 crystals. Among them, hydrothermal method seems to be a prevailing process for the preparation of uniform doped TiO_2 with various metal ions involved, including Ag^+,[13] Cd^{2+},[14] Mn^{2+} and Fe^{3+}.[15,16] However, there have been relatively few studies reported for the Ni-ion doped TiO_2 catalysts, while their photocatalytic activity is believed to be improved substantially once the optimal incorporation of Ni ions with TiO_2 matrix was achieved.[17] In particular, the lack of systematic investigations on Ni^{2+}-doped TiO_2 also impedes their practical applications for the removal of dye pollutants. Therefore, in this study, we explored the synthesis, characterization, and photocatalytic activity of TiO_2 with various contents of doped Ni^{2+} ions, prepared using an inexpensive, facile and reliable hydrothermal method. Two dominant azo dyes in wastewater from textile effluents, including Remazol Black 5 (RB5) and Remazol Brilliant Orange 3R (3R) dyes, were the targets for evaluating the photocatalytic performance of Ni^{2+}-doped TiO_2. Furthermore, extensive investigations of dominant factors effecting on the recycling utilization of these catalyst materials for the dye removal were also performed.

Experimental

Synthesis of Ni^{2+}-doped TiO_2

Department of Applied Materials and Optoelectronic Engineering, National Chi Nan University, Nantou 545, Taiwan. Email: timcychen@ncnu.edu.tw
† Electronic Supplementary Information (ESI) available

In a hydrothermal process, 0.01 mol of titanium(IV) isopropoxide was first dissolved in absolute ethanol (10 ml). Next, 0.01 mol of 1-Tetradecylamine and three various amount of $NiSO_4$ were added and gently stirred at 50°C for 10 min. Subsequently, the mixed solution was slowly dropped into 100 ml of distilled water under mechanical stirring with speed of 400 rpm and white TiO_2-based precipitates were grown hydrothermally. The mixtures were then stirred with mechanical stirring (800 rpm) for 1 h and followed by aging process at room temperature for 2 d in the dark. After cooling down, the mixtures were filtrated and rinsed with deionized (DI) water several times. Finally, the crystallization of Ni-doped TiO_2 was achieved by annealing process at 450 °C for 3 h. Here, three types of doped TiO_2 photocatalysts, including 0.5%, 1% and 5%-Ni^{2+} doped TiO_2,were prepared, respectively, where the contents of Ni ions were determined by the relative molar ratio (ρ) as bellow, $\rho = n_{Ni}/(n_{Ni}+n_{Ti}))x100\%$.

Characterizations

The crystalline structures of photocatalysts were characterized by a Rigaku Multiflex X-ray diffractometer using Cu-Kα radiation (λ = 1.5406 Å, 40 kV, and 40 mA). The morphologies and chemical compositions were investigated using scanning electron microscopy (SEM, Hitachi JSM-6390) and energy-dispersive X-ray (EDX) spectrometer (Oxford INCA 350), respectively. Prior to performing SEM observations, a thin layer of Au was deposited on sample surfaces to improving the imaging process. The absorption spectra of the photocatalysts were measured with a Jasco V-570 UV/VIS/NIR spectrophotometer equipped with an integrating sphere.

Adsorption isotherms of azo dyes

The adsorption equilibrium experiment was conducted by dispersing 10 mg of Ni^{2+}-doped TiO_2 nanoparticles into 10 ml DI water with various concentrations (0.05-0.40 mM) of target dyes. In each test, the pH value of mixed solution was controlled to be 2.0, and then stirred in the dark for 5 h at 30 °C. After that, the concentrations of dyes at each time interval were determined by the intensity of absorption peak at 597 nm (RB5 dye) and 494 nm (3R dye), respectively, using a UV/visible spectrophotometer (Shimadzu UV-2401 PC). The amount of adsorption (Q, mmol/g) was calculated by the equation as below,

$$Q = (C_i - C_t)V/W \quad (1)$$

where C_i and C_t represent the concentration of dyes measured at initial (t= 0) and certain reaction time (t= t). V is denoted as the volume of dye solution, and W is the weight of the photocatalysts.

Photocatalytic measurements

Evaluation of pohotcatalytic activity of Ni^{2+}-doped TiO_2 nanoparticles was conducted using a PanChum multilamp photoreactor (PR-2000) with switchable light sources. In each test, 10 mg of Ni^{2+}-doped TiO_2 photocatalysts were dispersed in 10 ml aqueous solution containing 0.2 mM of tested dyes in a 20 ml cylindrical quartz tube. The suspension was magnetically stirred in the dark for 1 hr before the light irradiation to establish the adsorption equilibrium. The photoreactor utilized in the photocatalytic experiments consists of eight sets of low-pressure quartz mercury lamps with monochromatic wavelengths of 254 nm, 306 nm, 365 nm and 580 nm, respectively. After the photocatalytic experiments, an aliquot of the solution (0.1 ml) at given time intervals (10min) was withdrawn from the reactor and diluted with 5 ml distilled water. The aqueous mixture was then analyzed using UV/visible spectrophotometer (Shimadzu UV-2401 PC). In general, the dye concentration was evaluated at wavelength of 597 nm for RB5 dye and at wavelength of 494 nm for 3R dyes, corresponding to the maximum absorption wavelength of RB5 and 3R dyes, respectively.

Results and discussion

Morphology, crystalline structure and optical property of Ni^{2+}-doped TiO_2

Fig. 1 presents the schematic illustration of process flow for the formation of Ni^{2+}-doped TiO_2 photocatalysts. Specifically, the hydrothermal process involves with four dominant steps: (i) Substitution of 1-Tetradecylamine and titanium(IV) isopropoxide; (ii) Hydrolysis reaction and followed by condensation process; (iii) Incorporations of Ni ions with TiO_2 lattice; (iv) Crystallization process through calcination of the samples. To characterize the as-prepared photocatalysts, morphology, crystallographic structure and light-absorption property were investigated. First, the morphologies of as-prepared Ni^{2+}-doped TiO_2 were examined through SEM observations, as shown in Fig. 2. All three synthesized Ni^{2+}-doped TiO_2, including 0.5%, 1% and 5% of Ni^{2+} doping, exhibit the sphere shapes with consistent distributions of diameter ranging from 200 to 400 nm. Notice that these round morphologies of formed nanoparticles are driven by the well incorporation of Ni ions with TiO_2 crystalline matrix [Fig. 1]. In fact, the uniform sphere-like nanoparticles can be only formed by the optimal introduction of 1-Tetradecylamine as surfactants during the hydrothermal process, whereas the insufficient amount of surfactants added to the reaction leads to the formation of arbitrary shape of TiO_2-based

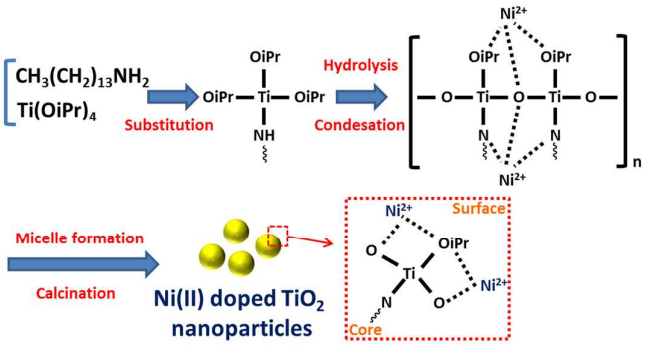

Fig. 1 Schematic illustrations of the procedures for the synthesis of Ni^{2+}-doped TiO_2 photocatalysts using a simple hydrothermal method.

On the other hand, while the shapes of doped TiO_2 are maintained, the surfaces of formed nanoparticles turn to be

rougher as the amount of introduced Ni ions increases, as shown in Figs. 2(a)-(c). These findings can be attributed to the incomplete hydrolysis and condensation process with Ni ions and TiO_2 lattice due to the excess amount of Ni ions involved. This is particularly apparent in the case of 5%-Ni^{2+} doped TiO_2, as shown in Fig. 2(c). In addition, the chemical composition of Ni ions in doped TiO_2 nanoparticles was also evaluated using EDS analysis, where the contents of Ni^{2+} doping, including 0.41 % (Fig. 2(a)), 0.89 % (Fig. 2(b)) and 5.35 % (Fig. 2(c)), match well with the designed values, 0.5 %, 1 % and 5 % of Ni^{2+} doping, respectively. Next, the crystalline phases of Ni^{2+}-doped samples, along with non-doped TiO_2, referred as pure TiO_2, were characterized with XRD analysis, as shown in Fig. 3(a). The similar diffraction patterns and corresponded crystal planes in these four cases can be observed, showing that the perfect anatase crystallographic phases are preserved regardless of the contents of Ni^{2+} doping. Fig. 3(b) further demonstrates the absorption characteristics of these four samples. Compared with pure TiO_2 which can only absorb light within UV region, the absorption edges of three Ni^{2+}-doped TiO_2 are extended toward near-IR region. In fact, the absorption bands are gradually enlarged with edge of 410 nm for 0.5% doping and 450 nm for 1% doping (insert of Fig. 3(b)), but substantially extended over 1400 nm for 5% doping, as shown in Fig. 3(b). The band gap energies of pure TiO_2, 0.5% Ni^{2+}-doped TiO_2 and 1% Ni^{2+}-doped TiO_2 are found to be 3.32 eV, 3.26 eV and 3.20 eV, respectively. Notice that the significant extension of absorption range in 5%-doped TiO_2 may be attributed to the occurrence of excess Ni ions or Ni clusters mixed with doped TiO_2, which therefore degrades their photocatalyitc activity. These issues will be further discussed later.

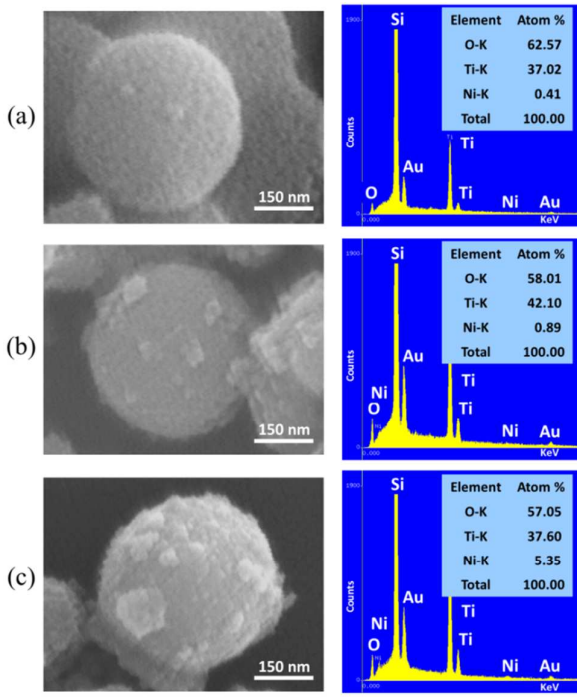

Fig. 2 Representative SEM images and corresponding EDS analysis of Ni^{2+}-doped TiO_2 with doping concentration of (a) 0.5%-Ni^{2+}, (b) 1%-Ni^{2+} and (c) 5%-Ni^{2+}. The EDS results confirmed that the Ni compositions of synthesized TiO_2 nanoparticles are well corresponded to the concentrations of Ni precursors used for catalyst preparation.

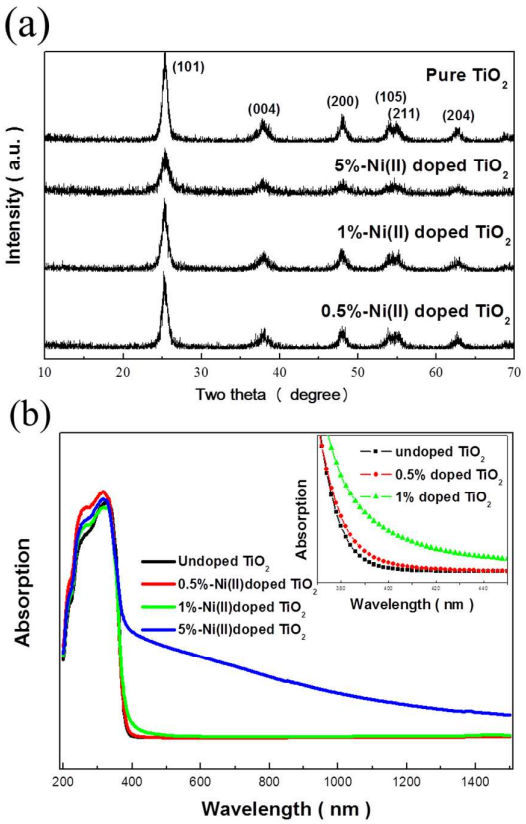

Fig. 3 (a) XRD patterns of four various TiO_2-based photocatalysts. (b) UV/Vis absorption spectra of non-doped TiO_2, 0.5%-Ni^{2+} doped TiO_2, 1%-Ni^{2+} doped TiO_2 and 5%-Ni^{2+} doped TiO_2, respectively.

Adsorption phenomena of dyes

Prior to testing the photocatalytic performance of prepared Ni^{2+}-doped TiO_2, it is pivotal to unveil the adsorption phenomena of dyes on the tested photocatalysts. To perform these experiments, two dominant and intensively used azo dyes, RB5 and 3R, were separately tested. The resulting adsorption isotherms, in terms of C_e versus Q_e are presented in Fig. 4(a), where C_e and Q_e represent the equilibrium concentration of dyes and equilibrium adsorption capacity of dyes, respectively. To further model the adsorption behaviors of these two kinds of dyes on Ni^{2+}-doped TiO_2, we extracted the measured data from Fig. 4(a) and re-plotted them with the relationship of C_e and C_e/Q_e, as presented in Fig. 4(b). Here, Langmuir isotherm model was employed for describing the dye adsorption on the Ni^{2+}-doped TiO_2, represented as below, [18,19]

$$C_e/Q_e = C_e/Q_m + 1/(Q_m K_L) \quad (2)$$

where Q_m is the maximum adsorption capacity of dyes. K_L represents the Langmuir adsorption equilibrium constant. As evidenced in Fig. 4(b), the clear linear fittings with correlation coefficient (R^2) in both RB5 (R^2= 0.99) and 3R dyes (R^2= 0.99)

suggest that the adsorption of these two dyes dominantly follow the Langmuir adsorption pathway.

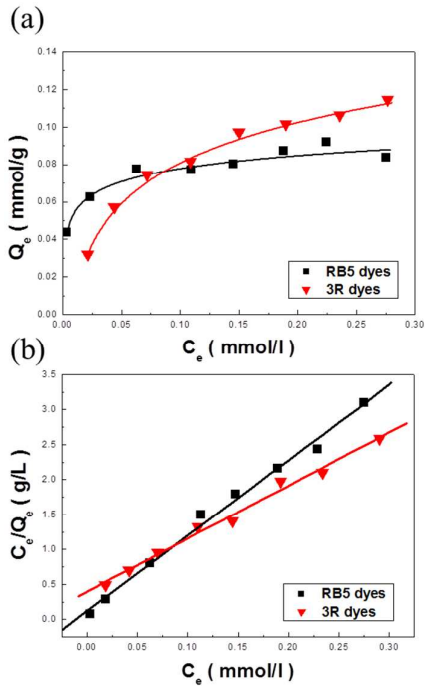

Fig. 4 (a) Adsorption isotherms of two kinds of azo dyes: RB5 and 3R in aqueous suspension of 1%-Ni^{2+} doped TiO_2 nanoparticles under following condition: catalyst loading= 1 mg/ml and temperature= 30 ^{0}C for 5 h. (b) Langmuir fittings of dye adsorption on 1%-Ni^{2+} doped TiO_2 photocatalysts.

Catalytic performance and kinetic study

To find out the optimum doping amount of Ni ions on TiO_2-based samples, the photocatalytic activity of various amount of Ni^{2+} doping, including 0.5%, 1% and 5%, were investigated, as presented in Figs. 5(a) and (b). Both RB5 (Fig. 5(a)) and 3R (Fig. 5(b)) dyes were tested to reveal the universal photocatalytic performance of our reported photocatalysts for the practical use of degrading azo dyes. From the comparisons of Figs. 5(a) and 5(b), it can be clearly observed that the doped TiO_2 with 1% Ni ions gives rise to the best photocatalytic activity for both RB5 and 3R dyes. Specifically, the remaining RB5 (3R) dyes after 100-min reaction are 10.1% (21.0%) in 0.5% of Ni^{2+} doping, 4.6% (9.2%) in 1% of Ni^{2+} doping, 14.7% (41.2%) in 5% of Ni^{2+} doping and 13.7% (32.1%) in pure TiO_2, respectively. The doping of Ni ions essentially facilitates the charge separation of photo-generated carriers, due to an electron donor level provided by the 3d orbitals of Ni ions, thus enhancing the dye-degradation activity.[17,20] Notice that the excess amount of Ni^{2+} doping appears in the case of 5%-Ni^{2+} doped TiO_2, where the additional Ni ions may behave as the recombination centers of photo-generated holes and electrons, thus suppressing the activity of photocatalysts for dye degradation.

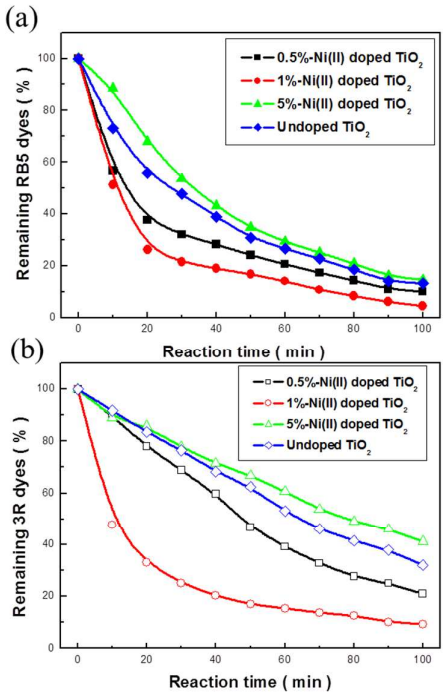

Fig. 5 Kinetic photodegradation of (a) RB5 and (b) 3R dyes in aqueous suspension in the presence of three different Ni^{2+}-doped and un-doped TiO_2 photocatalysts, respectively.

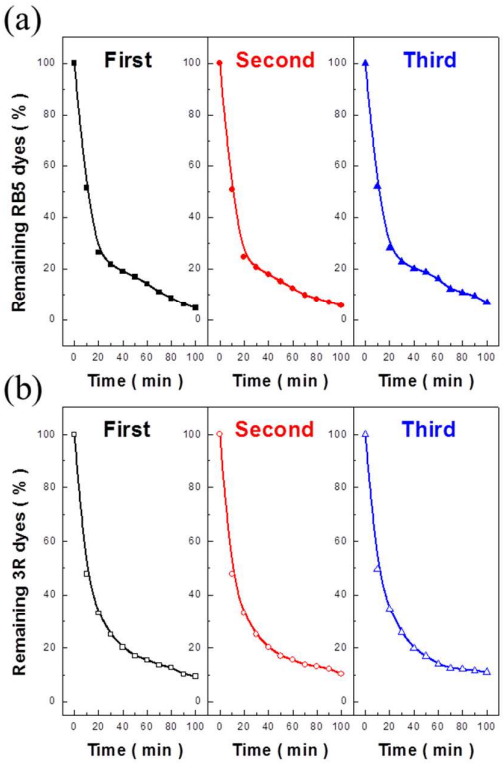

Fig. 6 (a) and (b) are the recycling tests of photocatalyst for the removal of RB5 and 3R dyes, respectively.

The recycling capability of 1%-Ni^{2+} doped TiO_2 catalysts were further tested, where three photocatalytic experiments were

performed subsequently, as shown in Figs. 6(a) and 6(b). The photodegradation curves, in terms of remaining dyes (%) versus reaction time (min) from these three tests are approximately consistent, for both RB5 (Fig. 6(a)) and 3R (Fig. 6(b)) dyes. These results evidence the fact that 1%-Ni^{2+} doped TiO_2 photocatalysts possess the reliable and robust photocatalyitc capability, and allow to being reused for the practical needs.

It has been reported that the loadings of photocatalysts for pollutant removal also affect their photocatalytic efficiency.[21] To unveil these issues, four different loadings of 1%-Ni^{2+} doped TiO_2 were tested for the removal of 0.2 mM of RB5 dyes. Likewise, similar experiments were performed in the presence of 3R dyes. The measured results are shown in Figs. 7(a) and 7(b), in which the efficiency of dye degradation increases with the introduction of more photocatalysts. Parallel to the effect of catalyst loadings, influences of dye concentrations (0.1, 0.2 and 0.3 mM) as well as illumination wavelengths (580, 352, 306 and 254 nm) were separately tested. The summarized results are presented in Figs. 8(a) and 8(b), showing that 1%-Ni^{2+} doped TiO_2 exhibits better photocatalytic activity for the degradation of RB5 dyes than 3R dyes. The possible reason is more effective adsorption of RB5 dyes on catalyst surfaces for standing on the photodegradation process.[22] Apart from that, 1%-Ni^{2+} doped TiO_2 are found to be efficient for both RB5 and 3R dyes with wide range of dye concentrations and broad wavelengths of illuminated light because of the enhanced absorption for long-wavelength lights, as evidenced in Fig. 3(b).

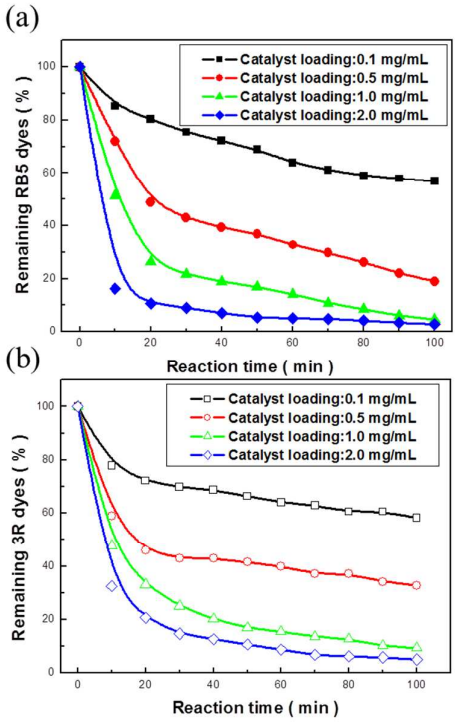

Fig. 7 Kinetic photodegradation of (a) RB5 and (b) 3R dyes in aqueous suspension in the presence of 1%-Ni^{2+} doped TiO_2 photocatalysts with different catalyst loadings, respectively.

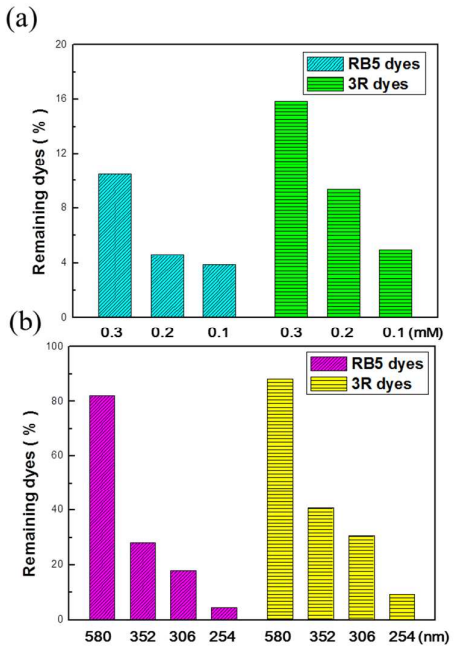

Fig. 8 Influences of (a) three various dye concentrations and (b) four various illumination wavelengths on the photocatalytic performance of 1%-Ni^{2+} doped TiO_2 photocatalysts, respectively.

Finally, to model the reaction kinetics on dye removal in the presence of 1%-Ni^{2+} doped TiO_2, the photocatalyitc experiments were performed at given time intervals during the time course of light illumination (0-100 min). Three possible kinetic models, including first-order kinetic model, second-order kinetic model and the Langmuir–Hinshelwood kinetic model were examined to envision the underlying photodegradation kinetics, as expressed below,

First-order kinetic model,[23,24]

$$\ln C_t = -k_1 t + \ln C_0 \quad (3)$$

Second-order kinetic model,[25]

$$1/C_t = k_2 t + 1/C_0 \quad (4)$$

Langumuir-Hinshelwood kinetic mode,[26]

$$\ln(C_t / C_0) + K_L(C_0 - C_t) = -k_3 K_L t \quad (5)$$

where C_0 and C_t are the concentration of dyes measured at initial (t= 0) and certain reaction time (t= t). k_1, k_2 and k_3 represent the first-order, second-order and Langmuir–Hinshelwood kinetic rate constants, respectively. K_L is the Langmuir absorption equilibrium constant. Figs. 9(a) and 9(b) present the kinetic modeling of these three universal expressions for both RB5 and 3R dyes. The correlation coefficient, R^2, was calculated from each kinetic model to validate the preferable mechanism for the dye degradation. It is clearly evidenced that the second-order model with the highest value of correlation coefficient in both RB5 (R^2= 0.95) and 3R (R^2= 0.96) among three tested models here, which can be regarded as the explicit mechanism of photocatalysis process using 1%-Ni^{2+} doped TiO_2. Based on that, the reaction constant (k_2) can be further estimated, where the values are 1.21 (g/mmol·min) for RB5 dyes and 0.66 (g/mmol·min) for 3R dyes. These quantitative results again correspond well to the

experimental data shown in Figs. 5 and 7, indicating that the degradation of RB5 dyes are kinetically favorable than that of 3R in the presence of 1%-Ni^{2+} doped TiO_2.

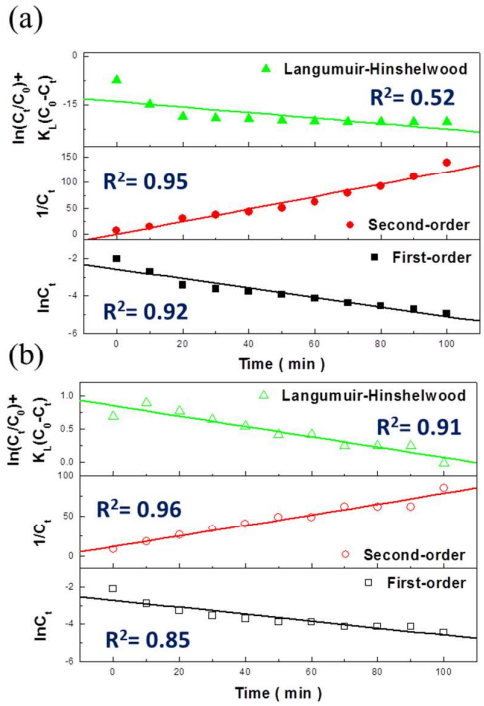

Fig. 9 Kinetic modeling of photocatalytic process on the degradation of (a) RB5 and (b) 3R dyes using 1%-Ni^{2+} doped TiO_2 photocatalysts.

Conclusionss

In conclusion, a simple and reliable hydrothermal method was reported to synthesize the Ni^{2+}-doped TiO_2. We explored the synthesis, characterization, adsorption behavior and photocatalytic activity of doped TiO_2 with various contents of doped Ni^{2+} ions. It is found that 1%-Ni^{2+} doped TiO_2 possess the degradation efficiency of 3 times for RB5 dyes and 3.5 times for 3R dyes higher than those of un-doped TiO_2. Furthermore, systematic investigations of several factors, including catalyst loadings, dye concentrations and illumination wavelengths were conducted, indicating the fact that the 1%-Ni^{2+} doped TiO_2 benefit both the superior photocatalyitc performance and robust recycling capability, and allow to being reused for the practical needs.

Acknowledgements

This study was financially supported by Ministry of Science and Technology of Taiwan under Contracts No. MOST 104-2628-E-260-001-MY2 and No. MOST 104-2623-E-260-001-D.

Notes and references

1 E. Forgacs, T. Cserhati and G. Oros, *Environ. Int.*, 2004, **30**, 953.
2 G. de Aragao Umbuzeiro, H. S. Freeman, S. H. Warren, D. P. de Oliveira, Y. Terao, T. Watanabe and L. D. Claxton, *Chemosphere*, 2005, **60**, 55.
3 I. K. Konstantinou and T. A. Albanis, *Appl. Catal. B*, 2004, **49**, 1.
4 A. Fujishima and K. Honda, *Nature*, 1972, **238**, 37.
5 M. A. Rauf, M. A. Meetani and S. Hisaindee, *Desalination*, 2011, **276**, 13.
6 K. Wilke and H. D. Breuer, *J. Photochem. Photobiol. A*, 1999, **121**, 49.
7 V. Subramanian, E. E. Wolf and P. V. Kamat, *Langmuir*, 2003, **19**, 469.
8 X. Xiang, L. Xie, Z. Li and F. Li, *Chem. Eng. J.*, 2013, **221**, 222.
9 W. He, Y. Yang, L. Wang, J. Yang, X. Xiang, D. Yan and F. Li, *ChemSusChem*, 2015, **8**, 1568.
10 Y. Zhu, L. Zhang, C. Gao, L. Cao, *J. Mater. Sci.*, 2000, **35**, 4049.
11 R. J. Tayade, R. G. Kulkarni and R. V. Jasra, *Ind. Eng. Chem. Res.*, 2006, **45**, 5231.
12 E. Hosono, S. Fujihara, K. Kakiuchi and H. Imai, *J. Am. Chem. Soc.*, 2004, **126**, 7790.
13 Y. Li, M. Ma, W. Chen, L. Li and M. Zen, *Mater. Chem. Phys.*, 2011, **129**, 501.
14 L. Andronic, A. Enesca, C. Vladuta and A. Duta, *Chem. Eng. J.*, 2009, **152**, 64.
15 L. G. Devi, N. Kottam, B. N. Murthy and S. G. Kumar, *J. Mol. Catal.*, 2010, **A328**, 44.
16 Z. Ambrus, N. Balazs, T. Alapi, G. Wittmann and P. Sipos, *Appl. Catal. B*, 2008, **81**, 27.
17 Z. Zou, J. Ye, K. Sayama and H. Arakawa, *Nature*, 2001, **414**, 625.
18 I. Langumuir, *J. Am. Chem. Soc.*, 1918, **40**, 1361.
19 K. Y. Foo and B. H. Hameed, *Chem. Eng. J.*, 2010, **156**, 2.
20 J. Choi, H. Park and M.R. Hoffmann, *J. Mater. Res.*, 2010, **25**,149.
21 R. L. Narayana, M. Matheswaran, A. A. Aziz and P. Saravanan, *Desalination*, 2011, **269**, 249.
22 E. Forgacs, T. Cserhatia and G. Oros, *Environ. Int.*, 2004, **30**, 953.
23 S. H. Kim, H. H. Ngo, H. K. Shon and S. Vigneswaran, *Sep. Purif. Technol.*, 2008, **58**, 335.
24 C. Y. Chen and Y. R. Liu, *Sci. Adv. Mater.*, 2015, **7**, 1053.
25 K. V. Kumara, K. Porkodib and A. Selvaganapathi, *Dyes Pigments*, 2007, **75**, 246.
26 J. M. Kesselman, N. S. Lewis and M. R. Hoffmann, *Environ. Sci. Technol.*, 1997, 31, 2298.

Graphical abstract

Kinetic study of self-assembly Ni(II)-doped TiO_2 nanocatalysts for the photodegradation of azo pollutants

Chia-Yun Chen* and Li-Jen Hsu
Department of Applied Materials and Optoelectronic Engineering, National Chi Nan University, Nantou 545, Taiwan